

Electronic structure of the mononuclear Ag(II) complex $[\text{Ag}([\text{18}] \text{aneS}_4\text{O}_2)]^{2+}$ ($[\text{18}] \text{aneS}_4\text{O}_2 = 1,10\text{-dioxo-4,7,13,16-tetrathiacyclooctadecane}$)[†]

Deguang Huang,^a Alexander J. Blake,^a Eric J. L. McInnes,^b Jonathan McMaster,^{*a} E. Stephen Davies,^a Claire Wilson,^a Joanna Wolowska^b and Martin Schröder^{*a}

Received (in Cambridge, UK) 14th November 2007, Accepted 19th December 2007

First published as an Advance Article on the web 17th January 2008

DOI: 10.1039/b717647c

The structure of $[\text{Ag}([\text{18}] \text{aneS}_4\text{O}_2)](\text{PF}_6)_2 \cdot \text{CH}_2\text{Cl}_2$ shows a highly unusual and unexpected boat conformation for the macrocycle with square-planar S_4 -coordination at the formal Ag(II) centre and the two ether O-centres lying on the same side of the S_4 plane; the SOMO in $[\text{Ag}([\text{18}] \text{aneS}_4\text{O}_2)]^{2+}$ possesses 22.7% Ag $4d_{xy}$ character, as determined by multi-frequency EPR spectroscopy and supported by DFT calculations.

Complexes incorporating formal Ag(II) centres have been used as oxidants in organic synthesis¹ and have been identified in radioactive waste processing.² The reported structures of mononuclear Ag(II) complexes are dominated by N-donor ligands of porphyrins,³ macrocycles,⁴ bipyridines⁵ and pyridine-2-carboxylate derivatives⁶ in which the metal centre is bound in a square-planar geometry with weak axial interaction(s) to counter-anions or co-ligands. Sulfur-based ligands⁷ and thioether macrocycles^{8,9} have also been used to complex redox-active Ag centres. However, crystal structures of mononuclear Ag(II) complexes with S-donor ligands remain very rare, the only reported example is the homoleptic thioether macrocyclic complex $[\text{Ag}([\text{18}] \text{aneS}_6)](\text{ClO}_4)_2$ ($[\text{18}] \text{aneS}_6 = 1,4,7,10,13,16\text{-hexathiacyclooctadecane}$).¹⁰ As part of our on-going studies of complexes containing unusual metal oxidation states,¹¹ we were interested in defining the extent to which homoleptic thioether coordination stabilises a formal Ag(II) centre. Thus, we modified the ligand donor set from S_6 to S_4O_2 -coordination *via* incorporation of two ether O-donors, and report herein the results of structural and electronic investigations of $[\text{Ag}([\text{18}] \text{aneS}_4\text{O}_2)](\text{PF}_6)_2$ ($[\text{18}] \text{aneS}_4\text{O}_2 = 1,10\text{-dioxo-4,7,13,16-tetrathiacyclooctadecane}$) for direct comparison with its $[\text{Ag}([\text{18}] \text{aneS}_6)](\text{ClO}_4)_2$ counterpart.¹⁰

$[\text{Ag}([\text{18}] \text{aneS}_4\text{O}_2)]\text{PF}_6$ was prepared by reaction of $[\text{18}] \text{aneS}_4\text{O}_2$ with AgPF_6 in $\text{CH}_2\text{Cl}_2\text{-MeOH}$, and a single crystal of $[\text{Ag}([\text{18}] \text{aneS}_4\text{O}_2)]\text{PF}_6 \cdot \text{MeCN}$ suitable for X-ray crystallography[‡] was obtained by diffusion of Et_2O into a solution

of the complex in MeCN at -20°C . There is minor disorder in the macrocyclic ring of one of the two independent cations in each asymmetric unit. The structure of the $[\text{Ag}([\text{18}] \text{aneS}_4\text{O}_2)]^+$ cation shows *meso* coordination of the macrocycle with four S-donors bound to Ag^{I} in a distorted tetrahedral coordination geometry with a dihedral angle of $70.0(2)^\circ$ between the planes defined by $\text{S}(4)\text{Ag}(1)\text{S}(7)$ and $\text{S}(13)\text{Ag}(1)\text{S}(16)$ consistent with a formal Ag(I) oxidation state in this complex [Fig. 1(a)]. The O-donors remain unbound to the Ag^{I} centre [$\text{Ag}(1) \cdots \text{O}(1)$ 3.092(3) and $\text{Ag}(1) \cdots \text{O}(10)$ 3.022(3) Å]. The Ag–S bond lengths [$\text{Ag}(1)\text{-S}(4)$ 2.5746(11), $\text{Ag}(1)\text{-S}(7)$ 2.6094(13), $\text{Ag}(1)\text{-S}(13)$ 2.5745(11) and $\text{Ag}(1)\text{-S}(16)$ 2.5724(11) Å] in $[\text{Ag}([\text{18}] \text{aneS}_4\text{O}_2)]^+$ are shorter than the Ag–S bond lengths [2.6665(12) and 2.7813(10) Å] in $[\text{Ag}([\text{18}] \text{aneS}_6)]^+$ consistent⁹ with the lower coordination number of $[\text{Ag}([\text{18}] \text{aneS}_4\text{O}_2)]^+$.

The cyclic voltammogram of $[\text{Ag}([\text{18}] \text{aneS}_4\text{O}_2)]\text{PF}_6$ in CH_2Cl_2 containing 0.4 M NBu_4PF_6 at a scan rate of 100 mV s^{-1} shows an oxidative process at $E_p^{\text{a}} = +1.09$ V vs. Fc^+/Fc at 253 K with a return wave observed at $E_p^{\text{c}} = +0.95$ V ($\Delta E = 140$ mV) (see ESI[†]). This contrasts with the fully irreversible process with no return wave observed at $E_p^{\text{a}} = +0.93$ V for $[\text{Ag}([\text{18}] \text{aneS}_6)]\text{PF}_6$ under the same experimental conditions. This suggests a degree of increased kinetic inertness for Ag(II) with the $[\text{18}] \text{aneS}_4\text{O}_2$ macrocycle. In addition, the general broadening of the cyclic voltammogram response for $[\text{Ag}([\text{18}] \text{aneS}_4\text{O}_2)]\text{PF}_6$ is consistent with changes in coordination at the metal centre upon oxidation. Coulometric measurements at

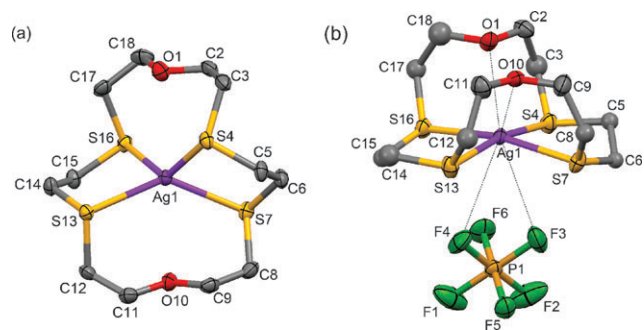


Fig. 1 (a) View of one of the two crystallographically independent $[\text{Ag}([\text{18}] \text{aneS}_4\text{O}_2)]^+$ cations in the asymmetric unit. (b) View of $[\text{Ag}([\text{18}] \text{aneS}_4\text{O}_2)]^{2+}$ showing interactions with O-donor atoms and with PF_6^- anion in the solid state. One of the two equally-occupied disorder components of the atoms C3, C5, C6, C8, C12, C14, C15, C17 and C18 in the macrocyclic ring is omitted for clarity.

^a School of Chemistry, University of Nottingham, Nottingham, UK NG7 2RD. E-mail: M.Schroder@nottingham.ac.uk; J.McMaster@nottingham.ac.uk

^b EPSRC Multi-Frequency EPR Centre, School of Chemistry, University of Manchester, Manchester, UK M13 9PL

[†] Electronic supplementary information (ESI) available: Synthesis and structural data of Ag(I) and Ag(II), cyclic voltammograms of $[\text{Ag}([\text{18}] \text{aneS}_4\text{O}_2)]\text{PF}_6$ and $[\text{Ag}([\text{18}] \text{aneS}_6)]\text{PF}_6$, EPR physical measurements and EPR theoretical calculation, experimental details of DFT calculations. See DOI: 10.1039/b717647c

+ 1.12 V vs. Fc⁺/Fc confirm that the oxidation of [Ag([18]aneS₄O₂)]PF₆ is a one-electron process, but this quantitative oxidation is accompanied by precipitation of the product during the course of the bulk experiment. Controlled potential electrolysis in a thin quartz cell (40 × 10 × 0.5 mm³) at +1.12 V vs. Fc⁺/Fc in CH₂Cl₂ containing 0.4 M NBu₄PF₆ under Ar at 253 K provided a route for the electrocrystallisation of [Ag([18]aneS₄O₂)](PF₆)₂·CH₂Cl₂ as blue needle crystals. These crystals, suitable for X-ray crystallography,[‡] were deposited on the surface of the Pt/Rh gauze working electrode after ca. 1 h of electrolysis.

The single-crystal X-ray structure of [Ag([18]aneS₄O₂)](PF₆)₂·CH₂Cl₂ [Fig. 1(b)] shows a highly unusual and unexpected boat conformation for the [18]aneS₄O₂ macrocycle that is significantly different from the structure of the parent [Ag([18]aneS₄O₂)]PF₆·MeCN complex. The majority of the macrocyclic carbon atoms are each disordered over two alternative sites, a common feature in cyclic thioether complexes. The Ag centre in [Ag([18]aneS₄O₂)](PF₆)₂·CH₂Cl₂ possesses a primary square-planar S₄-coordination sphere with the Ag–S distances [Ag(1)–S(4) 2.487(4), Ag(1)–S(7) 2.537(4), Ag(1)–S(13) 2.501(4), Ag(1)–S(16) 2.518(4) Å] significantly shorter than those in six-coordinated [Ag([18]aneS₆)](ClO₄)₂ [Ag(1)–S(1) 2.569(7), Ag(1)–S(2) 2.720(6) Å],¹⁰ consistent with the lower coordination number in the former complex. Interestingly and unusually, the two macrocyclic O-donors in [Ag([18]aneS₄O₂)](PF₆)₂ are located in *cis*-positions relative to the S₄-plane [Ag(1)···O(1) 2.814(9), Ag(1)···O(10) 2.797(10) Å] rather than in the expected *trans*-positions as observed in [Ag([18]aneS₄O₂)]PF₆ (see above).¹⁰ In [Ag([18]aneS₄O₂)](PF₆)₂, the Ag(II) ion lies 0.26 Å out of the least-squares S₄ plane of the macrocycle and towards the O-centres with one of the PF₆[−] counter-anions occupying a site below the cation [Ag–F 3.295(13) and 3.240(12) Å] on the opposite side of the S₄ plane to the macrocyclic ether centres. Thus, although the primary coordination at Ag(II) is square-planar *via* binding four thioether S-donors of the macrocycle, there is some evidence, at least in the solid state, of potential long-range interactions with ether O-donors and two F centres in the PF₆[−] anion to give a twist square-prismatic stereochemistry [Fig. 1(b)].

We have shown previously that high-valent transition metal complexes of thioether crowns are stabilised in acidic solutions.¹² Therefore, this approach was used to stabilise [Ag([18]aneS₄O₂)]²⁺ in solution to facilitate spectroscopic studies. Electrochemically prepared microcrystals of [Ag([18]aneS₄O₂)](PF₆)₂·CH₂Cl₂ were dissolved in 70% HClO₄ and the resultant sample was studied by multi-frequency EPR spectroscopy in fluid (293 K, X-band) and frozen solutions (125 K, S-, X- and Q-band, Fig. 2). The fluid-solution X-band spectrum of [Ag([18]aneS₄O₂)]²⁺ shows a doublet that results from hyperfine coupling to ^{107,109}Ag nuclei (^{107,109}Ag *I* = 1/2, 100% combined natural abundance) and simulation gave *g*_{iso} = 2.0273 and |*A*_{iso}| = 34 × 10^{−4} cm^{−1} [Fig. 2(a)]. The frozen-solution Q-band spectrum is axial with ^{107,109}Ag hyperfine that is clearly resolved in the *g*_{||} and *g*_⊥ regions [Fig. 2(d)]. Simulation of this spectrum gave *g*_⊥ = 2.0163, *g*_{||} = 2.0415; |*A*_⊥| = 31 × 10^{−4} cm^{−1} and |*A*_{||}| = 43 × 10^{−4} cm^{−1}. These spin Hamiltonian parameters were verified

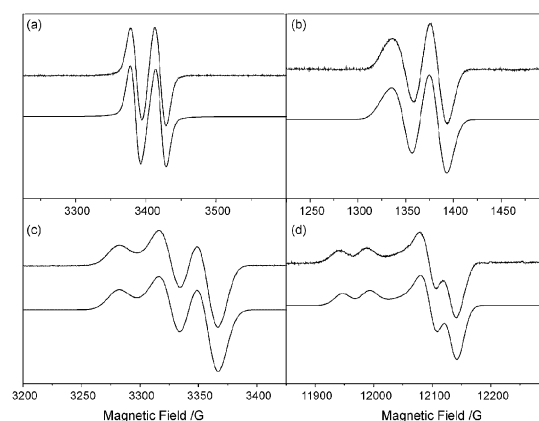


Fig. 2 Multi-frequency EPR spectra of [Ag([18]aneS₄O₂)]²⁺ in 70% HClO₄ solution. (a) X-Band fluid spectrum at 293 K (top) and simulation (bottom) with *g*_{iso} = 2.0273, |*A*_{iso}| = 34 × 10^{−4} cm^{−1}; (b) S-band frozen spectrum; (c) X-band frozen spectrum; (d) Q-band frozen spectrum at ca. 125 K (top) and simulations (bottom) with *g*₁₁ = *g*₂₂ = 2.0163, *g*₃₃ = 2.0415; |*A*₁₁| = |*A*₂₂| = 31 × 10^{−4} cm^{−1}, |*A*₃₃| = 43 × 10^{−4} cm^{−1}. Gaussian linewidths of *W*_{iso} = 14 × 10^{−4} cm^{−1} for X-band fluid spectrum; *W*₁₁ = *W*₂₂ = *W*₃₃ = 25 × 10^{−4} cm^{−1} for Q-band frozen spectrum; *W*₁₁ = *W*₂₂ = *W*₃₃ = 17 × 10^{−4} cm^{−1} for X- and S-band frozen spectra.

by the simultaneous simulation of the frozen-solution S- and X-band spectra [Fig. 2(b) and (c)]. The simulated hyperfine coupling constants require the sign of the *A* values to be either all positive or negative such that *A*_{iso} = (*A*_{||} + 2*A*_⊥)/3.

The axial EPR spectra of [Ag([18]aneS₄O₂)]²⁺ are consistent with the approximate square-planar molecular structure determined by X-ray crystallography. Thus, the *z*-axis was defined as being perpendicular to the S₄ plane with *g*_{||} and *A*_{||} lying along this axis, with the *x*-axis defined as pointing along the bisector of the S(4)–Ag(1)–S(16) angle. Thus, crystal-field theory predicts a 4d_{xy}-based SOMO in [Ag([18]aneS₄O₂)]²⁺ consistent with the observed *g*_{||} > *g*_⊥ > *g*_c pattern in the EPR spectra of the complex. Analysis of the simulated *g* and *A*-values from the multi-frequency EPR spectra gave α² = 22.7% with *A*_{zz} ≡ *A*_{||} and *g*_{zz} = *g*_{||} (see ESI[†]). Negative *A*-values gave invalid negative values for α². Thus, the contribution of 4d_{xy} metal orbital to the SOMO is 22.7% as determined by multi-frequency EPR spectroscopy.

The experimentally determined composition of the SOMO was compared with that determined by unrestricted relativistic DFT calculations (see ESI[†]). These calculations were carried out using the Amsterdam Density Functional (ADF) suite version 2005.01.^{13,14} An unconstrained model, based on the crystallographic structure of [Ag([18]aneS₄O₂)]²⁺, converged to a similar geometry but with Ag–S bond lengths that are on average 0.07 Å longer than those in the experimental structure. In contrast the Ag···O distances for the calculated geometry are 0.12 Å shorter than in the experimental structure, which may point towards a weak interaction involving the O-donors in this complex that may be associated with the displacement of the Ag ion out of the S₄ plane (see above). It is likely that the principal differences between the calculated and experimental geometries result from the omission of a weakly bound PF₆[−] counter-anion in the model employed for the calculations.

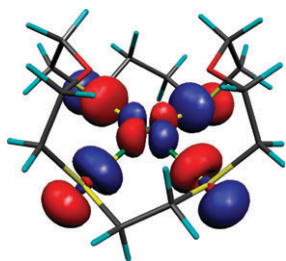


Fig. 3 Isosurface plot of the α -spin SOMO of $[\text{Ag}([18]\text{aneS}_4\text{O}_2)]^{2+}$ derived from a BP-TZP relativistic DFT calculation.

The calculated composition of the SOMO is 18.4% Ag $4d_{xy}$ and 68.4% S 3p (Fig. 3). The calculated Ag $4d_{xy}$ contribution is 4.3% less than that derived from the EPR spectroscopic studies; a similar difference was also observed for $[\text{Ag}([18]\text{aneS}_6)]^{2+}$,¹⁰ for which the calculated SOMO possesses 22% Ag $4d_{xy}$ character and EPR spectroscopic studies reveal a SOMO composition of 26% Ag $4d_{xy}$. Our spectroscopic and theoretical studies point to a slightly (4%) lower metal composition of the SOMO in $[\text{Ag}([18]\text{aneS}_4\text{O}_2)]^{2+}$ than $[\text{Ag}([18]\text{aneS}_6)]^{2+}$, and that the equatorial S-donors are capable of buffering these differences in the Ag contributions to the SOMO. It is interesting to note that the average in-plane Ag–S distance for $[\text{Ag}([18]\text{aneS}_4\text{O}_2)]^{2+}$ is 5% shorter than for $[\text{Ag}([18]\text{aneS}_6)]^{2+}$ suggesting greater Ag–S orbital overlap, and potentially greater covalency.

In summary, we have prepared $[\text{Ag}([18]\text{aneS}_4\text{O}_2)](\text{PF}_6)_2$ and shown that the macrocycle binds to the Ag(II) centre in a unique conformation. EPR spectroscopic and theoretical calculations on this complex show that $[\text{Ag}([18]\text{aneS}_6)]^{2+}$ and $[\text{Ag}([18]\text{aneS}_4\text{O}_2)]^{2+}$ possess similar Ag $4d_{xy}$ ground-states with significant spin density on the equatorial thioether S-donors. These results imply an overriding importance for equatorial thioether coordination in the stabilization of Ag(II) by crown thioether macrocycles. This notwithstanding, long-range interactions at and around axial sites with O-centres and PF_6^- anion may stabilize the formal Ag(II) centre in $[\text{Ag}([18]\text{aneS}_4\text{O}_2)]^{2+}$ in the solid state, although no Ag...F coupling was observed in solution by EPR spectroscopy.

We thank the EPSRC and the University of Nottingham for support and funding. D. H. gratefully acknowledges receipt of a Madam Chen Zhili Fellowship. We also thank STFC for access to Station 16.2smx on the Daresbury SRS and Dr T. J. Prior for experimental assistance. M. S. gratefully acknowledges receipt of a Royal Society Wolfson Merit Award and of a Royal Society Leverhulme Trust Senior Research Fellowship. We thank the EPSRC CW-EPR Service at The University of Manchester.

Notes and references

† Crystal data: $\text{C}_{14}\text{H}_{27}\text{NO}_2\text{S}_4\text{PF}_6\text{Ag}$, $M = 622.45$, orthorhombic, space group $Pna2_1$, $a = 21.0076(4)$, $b = 17.5973(6)$, $c = 12.5610(7)$ Å, $V = 4643.5(3)$ Å³, $T = 150(2)$ K, $Z = 8$, $D_c = 1.781$ g cm⁻³, 11085 unique reflections ($R_{\text{int}} = 0.0282$), final $R_1[F > 2\sigma(F)] = 0.030$, wR_2 (all data) = 0.0705.
 $\text{C}_{13}\text{H}_{26}\text{O}_2\text{S}_4\text{Cl}_2\text{P}_2\text{F}_{12}\text{Ag}$, $M = 811.29$, monoclinic, space group $P2_1/n$ (alt. $P2_1/c$, no. 14), $a = 11.190(2)$, $b = 10.510(2)$, $c = 22.990(5)$ Å,

$\beta = 91.00(3)^\circ$, $V = 2703.4(9)$ Å³, $T = 150(2)$ K, $Z = 4$, $D_c = 1.993$ g cm⁻³, 4733 unique reflections ($R_{\text{int}} = 0.177$). Application of disorder modelling and distance restraints to the macrocyclic C and solvent Cl atoms led to stable refinement and final $R_1[F > 2\sigma(F)] = 0.0944$, wR_2 (all data) = 0.251.

CCDC 667819 and 667820. For crystallographic data in CIF or other electronic format see DOI: 10.1039/b717647c

- (a) H. N. Po, *Coord. Chem. Rev.*, 1976, **20**, 171; (b) E. Mentasti, C. Baiocchi and J. S. Coe, *Coord. Chem. Rev.*, 1984, **54**, 131.
- J. C. Farmer, F. T. Wang, R. A. Hawley-Fedder, P. R. Lewis, L. J. Summers and L. Foiles, *J. Electrochem. Soc.*, 1992, **139**, 654.
- (a) G. D. Dorough, J. R. Miller and F. M. Huennekens, *J. Am. Chem. Soc.*, 1951, **73**, 4315; (b) W. R. Scheidt, J. U. Mondal, C. W. Eigenbrot, A. Adler, L. J. Radonovich and J. L. Hoard, *Inorg. Chem.*, 1986, **25**, 795; (c) W.-K. Wong, L. Zhang, W.-T. Wong, F. Xue and T. C. W. Mak, *J. Chem. Soc., Dalton Trans.*, 1999, 615; (d) T. Ishii, N. Aizawa, R. Kanehama, M. Yamashita, H. Matsuzaka, T. Kodama, K. Kikuchi and I. Ikemoto, *Inorg. Chim. Acta*, 2001, **317**, 81; (e) N. Aizawa, H. Hara, T. Ishii, M. Yamashita, H. Miyasaka, H. Matsuzaka, T. Kodama, K. Kikuchi and I. Ikemoto, *Mol. Cryst. Liq. Cryst. Sci. Technol. Sect. A*, 2002, **376**, 13.
- (a) K. B. Mertes, *Inorg. Chem.*, 1978, **17**, 49; (b) T. Ito, H. Ito and K. Toriumi, *Chem. Lett.*, 1981, 1101; (c) H. N. Po, E. Brinkman and R. J. Doedens, *Acta Crystallogr., Sect. C*, 1991, **47**, 2310; (d) H. N. Po, S.-C. Shen and R. J. Doedens, *Acta Crystallogr., Sect. C*, 1993, **49**, 1914; (e) Q.-M. Wang and T. C. W. Mak, *Chem. Commun.*, 2001, 807; (f) Q.-M. Wang, H. K. Lee and T. C. W. Mak, *New J. Chem.*, 2002, **26**, 513; (g) T. K. Kundu and P. T. Manoharan, *Mol. Phys.*, 2000, **98**, 2007.
- (a) G. W. Bushnell and M. A. Kahn, *Can. J. Chem.*, 1972, **50**, 315; (b) J. L. Atwood, M. L. Simms and D. A. Zatkan, *Cryst. Struct. Commun.*, 1973, **2**, 279.
- (a) M. G. B. Drew, R. W. Matthews and R. A. Walton, *J. Chem. Soc. A*, 1970, 1405; (b) M. G. B. Drew, R. W. Matthews and R. A. Walton, *J. Chem. Soc. A*, 1971, 2959.
- W. Levason and M. D. Spicer, *Coord. Chem. Rev.*, 1987, **76**, 45.
- (a) H.-J. Küppers, K. Wieghardt, Y.-H. Tsay, C. Krüger, B. Nuber and J. Weiss, *Angew. Chem., Int. Ed. Engl.*, 1987, **26**, 575; (b) P. J. Blower, J. A. Clarkson, S. C. Rawle, J. R. Hartman, R. E. Wolf, R. Yagbasan, S. G. Bott and S. R. Cooper, *Inorg. Chem.*, 1989, **28**, 4040; (c) A. J. Blake, R. O. Gould, G. Reid and M. Schröder, *J. Chem. Soc., Chem. Commun.*, 1990, 974; (d) A. J. Blake, G. Reid and M. Schröder, *J. Chem. Soc., Dalton Trans.*, 1991, 615; (e) A. J. Blake, D. Collison, R. O. Gould, G. Reid and M. Schröder, *J. Chem. Soc., Dalton Trans.*, 1993, 521; (f) M. Kampf, J. Griebel and R. Kirmse, *Z. Anorg. Allg. Chem.*, 2004, **630**, 2669.
- A. J. Blake, R. O. Gould, A. J. Holder, T. I. Hyde and M. Schröder, *Polyhedron*, 1989, **8**, 513.
- (a) J. L. Shaw, J. Wolowska, D. Collison, J. A. K. Howard, E. J. L. McInnes, J. McMaster, A. J. Blake, C. Wilson and M. Schröder, *J. Am. Chem. Soc.*, 2006, **128**, 13827; for a Ag(II) polynuclear S-donor complex, see; (b) R. Y. C. Shin, G. K. Tan, L. L. Koh and J. J. Vittal, *Organometallics*, 2005, **24**, 539.
- (a) J. Lewis and M. Schröder, *J. Chem. Soc., Dalton Trans.*, 1982, 1085; (b) C. W. G. Ansell, J. Lewis, P. R. Raithby, J. N. Ramsden and M. Schröder, *J. Chem. Soc., Chem. Commun.*, 1982, 546; (c) A. J. Blake, R. O. Gould, T. I. Hyde and M. Schröder, *J. Chem. Soc., Chem. Commun.*, 1987, 431; (d) A. J. Blake, A. J. Holder, T. I. Hyde and M. Schröder, *J. Chem. Soc., Chem. Commun.*, 1989, 1433; (e) A. J. Blake, G. Reid and M. Schröder, *J. Chem. Soc., Dalton Trans.*, 1990, 3363.
- A. J. Blake, A. J. Holder, T. I. Hyde, H.-J. Küppers, M. Schröder, S. Stötzel and K. Wieghardt, *J. Chem. Soc., Chem. Commun.*, 1989, 1600.
- C. F. Guerra, J. G. Snijders, G. te Velde and E. J. Baerends, *Theor. Chem. Acc.*, 1998, **99**, 391.
- G. te Velde, F. M. Bickelhaupt, S. J. A. van Gisbergen, C. F. Guerra, E. J. Baerends, J. G. Snijders and T. Ziegler, *J. Comput. Chem.*, 2001, **22**, 931.